

Ultra-fast excited state dynamics in green fluorescent protein: Multiple states and proton transfer

MITA CHATTORAJ, BRETT A. KING, GEROLD U. BUBLITZ, AND STEVEN G. BOXER[†]

Department of Chemistry, Stanford University, Stanford, CA 94305-5080

Communicated by Michael Kasha, Florida State University, Tallahassee, FL, May 10, 1996 (received for review December 26, 1995)

ABSTRACT The green fluorescent protein (GFP) of the jellyfish *Aequorea Victoria* has attracted widespread interest since the discovery that its chromophore is generated by the autocatalytic, posttranslational cyclization and oxidation of a hexapeptide unit. This permits fusion of the DNA sequence of GFP with that of any protein whose expression or transport can then be readily monitored by sensitive fluorescence methods without the need to add exogenous fluorescent dyes. The excited state dynamics of GFP were studied following photo-excitation of each of its two strong absorption bands in the visible using fluorescence upconversion spectroscopy (about 100 fs time resolution). It is shown that excitation of the higher energy feature leads very rapidly to a form of the lower energy species, and that the excited state interconversion rate can be markedly slowed by replacing exchangeable protons with deuterons. This observation and others lead to a model in which the two visible absorption bands correspond to GFP in two ground-state conformations. These conformations can be slowly interconverted in the ground state, but the process is much faster in the excited state. The observed isotope effect suggests that the initial excited state process involves a proton transfer reaction that is followed by additional structural changes. These observations may help to rationalize and motivate mutations that alter the absorption properties and improve the photo stability of GFP.

The green fluorescent protein (GFP) of the jellyfish *Aequorea Victoria* has attracted widespread interest since the discovery that its chromophore is generated by the autocatalytic, post-translational cyclization and oxidation of a hexapeptide unit at positions 64–69 (1, 2). We have investigated the electronic absorption and ultra-fast emission from GFP and have discovered surprisingly rich photophysics and photochemistry, interesting in their own right and relevant to applications and modifications of this system.

The recent interest in this protein builds on many years of effort. The precise chromophore structure and conformation are still subject to investigation, and a three-dimensional structure of the protein is not yet available (3). The chromophore absorption in the visible region consists of two broad bands shown in Fig. 1A. Although these two bands could correspond to transitions from the ground to the first and second singlet excited states of the same chromophore, their ratio depends on conditions such as pH, temperature, and ionic strength (4) suggesting that two different, interconvertible forms of the chromophore may be present. By examining the excited state dynamics of the chromophore, both in its native state and following deuterium exchange, we demonstrate that two different forms are present and that their interconversion in the excited state depends on proton motion. Because GFP fluorescence is insensitive to oxygen quenching, it has been suggested that the chromophore is in a solvent inaccessible region (5). The fluorescence is stable in a variety

of harsh environments (temperature up to 70°C, pH 6–12, detergents, proteolysis, and kaotropic reagents) (6). Circular dichroism studies indicate that the secondary structure of the protein environment is necessary for fluorescence (7). Importantly, denaturation results in the total loss of the green fluorescence. Upon renaturation, the native fluorescence is restored (8); thus, the loss of fluorescence cannot be ascribed to bond-breaking, but must involve a conformational change of the chromophore (e.g., breaking conjugation) or a change in some significant interaction between the chromophore and the protein environment. Several single and multiple mutants of GFP have been prepared that possess shifted absorption and fluorescence spectra (1, 9, 10). Some of these mutations are distant in primary sequence from residues 64–69 (1), indicating that the chromophore is very sensitive to its environment and making this a fascinating system for investigating spectroscopy in an ordered system.

EXPERIMENTAL PROCEDURES

Recombinant GFP was produced in *Escherichia coli* by the methods of Chalfie *et al.* (11) except that the cells were grown at room temperature. The crude GFP was purified by column chromatography using DEAE cellulose and a linear gradient of NaCl (0 to 1 M) in 10 mM sodium phosphate buffer at pH 6.5. The fractions having a 286–397 nm absorbance ratio of two or less were pooled. All GFP samples were in 50% glycerol/50% water (vol/vol) at pH 6.5 in 10 mM phosphate buffer so they could be studied over a wide temperature range. Exchangeable protons were replaced by deuterium by diluting the protein with 10 mM phosphate buffer in D₂O at pH 6.5 (the pH meter is uncorrected for the isotope effect), then concentrating the sample to a minimum volume, and repeating this process three times. The resulting partially deuterated protein is denoted GFP-D and was diluted with glycerol whose hydroxyl protons had been exchanged for deuterium. The GFP samples were in this medium for several hours at room temperature and 48 hr at –20°C before data were taken.

Steady-state fluorescence spectra were measured using a SPEX fluorimeter, which was calibrated using a standard lamp. Instrument sensitivity to anisotropy measurements was tested using fluorescein in 90% glycerol/10% water mixture and comparing it to published results (12). Low temperature absorption and Stark effect spectra were measured and analyzed as described (13). The time evolution of the fluorescence up to 150 ps after excitation was measured by fluorescence upconversion using a setup that is described in ref. 14. The samples were excited by the second harmonic of an argon-ion-pumped Ti:sapphire laser. The laser fundamental had a pulse duration of 70 fs and a spectral bandwidth of 191 cm⁻¹, which is 30% higher than the theoretical Fourier transform limit; the second harmonic had a spectral bandwidth of 245 cm⁻¹. The cross-correlation of the frequency-doubled output scattering off the sample and the first harmonic used for

The publication costs of this article were defrayed in part by page charge payment. This article must therefore be hereby marked “advertisement” in accordance with 18 U.S.C. §1734 solely to indicate this fact.

Abbreviation: GFP, green fluorescent protein.
[†]To whom reprint requests should be addressed.

fluorescence mixing was used as the instrument response function. Its full width at half maximum was typically 160 fs. Ten milliwatts of light was used to excite the sample at 82 MHz. The excitation light was polarized at the magic angle with respect to the detection axis so that the data were not affected by molecular rotation. For room temperature studies, a 1-mm path-length quartz cuvette was used with rapid stirring by a small magnetic stir bar. The sample cuvette was translated between each scan of the delay line (i.e., every 1–2 min). A miniature Joule Thompson refrigerator (MMR Technologies, Mountain View, CA) was used to obtain lower temperatures (80–230 K) (14). The data sets were analyzed by convoluting the instrument response function with a model function composed of at most three exponentials, a baseline, and a time offset. Emission at wavelengths exhibiting a rise have exponential components with negative amplitudes. The parameters of the model function were fit to the collected data by minimizing χ^2 , which was typically less than 1.2 per degree of freedom.

RESULTS

Electronic Absorption. The room temperature and 77 K electronic absorption spectra of GFP are shown in Fig. 1. The room temperature profile shows two peaks absorbing at 478 nm (20,940 cm^{-1}) and 398 nm (25,160 cm^{-1}). At 77 K the higher energy peak shifts to lower energy, the lower energy peak shifts to higher energy, and the spectrum becomes significantly more structured. There was no effect of deuterating exchangeable protons on the absorption spectrum at either temperature (data not shown), indicating that exchanging protons with deuterium has no observable effect on the protein conformation or the vibrational structure of the chromophore.

Stark Effect. The Stark effect spectrum was used for obtaining information on the change in dipole moment, $\Delta\mu$, associated with the ground to excited state transitions. Fig. 2 shows the absorption (*A*) and Stark (*B*) spectra of GFP at 77 K. Under these conditions, the Stark spectrum is expected to

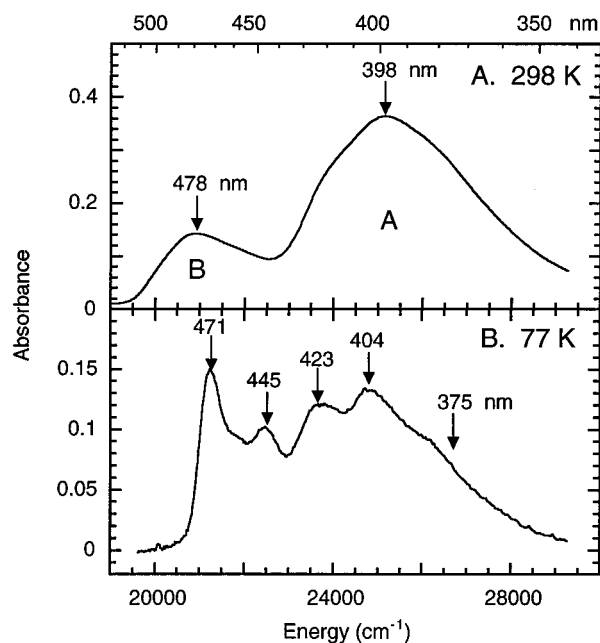


FIG. 1. Absorption spectrum of GFP in 50% glycerol/50% buffer (pH 6.5, 10 mM phosphate) at 298 K (*A*) and 77 K (*B*). Note that the spectra are plotted in linear energy units; units in nanometers are indicated on the upper horizontal axis. Arrows indicate excitation wavelengths for fluorescence data.

resemble the second derivative of the absorption (i.e., the band is broadened by application of an electric field) if the Stark effect is dominated by $\Delta\mu$. Comparison of the Stark spectrum with the second derivative in Fig. 2C shows that they are very similar; a quantitative analysis gives $|\Delta\mu| = 6.8 \pm 0.3 \text{ D}/f$, where f is the local field correction factor (typically around 1.1), and the angle ζ between the transition moment and $\Delta\mu$ is $21 \pm 7^\circ$. Note that the absorption band at higher energy does not contribute significantly to either the Stark spectrum or second derivative because the band is so broad. $|\Delta\mu|$ must be less than 20 D for this band or it would have been detected in the Stark spectrum. Simultaneous fitting of the absorption and Stark spectra shows that the low temperature absorption spectrum can be modeled by two overlapping bands, as shown in Fig. 2A. The lower energy band exhibits a well-resolved vibronic progression, readily seen in the Stark spectrum, with features separated by 1100–1250 cm^{-1} ; the higher energy band is featureless. Anticipating the results below, the ground and excited states associated with the higher energy band will be denoted A and A*; the states associated with the lower energy band will be called B and B*.

Steady-State Fluorescence. The room temperature fluorescence spectrum of GFP is relatively insensitive to excitation wavelength (data not shown). Small differences are observed: the spectrum obtained by exciting the higher energy absorption band at 398 nm is slightly more structured and narrower than the one obtained by exciting the lower energy band at 478 nm; also, excitation at 398 nm produces weak, unstructured emission in the 420–470 nm region. The room temperature emis-

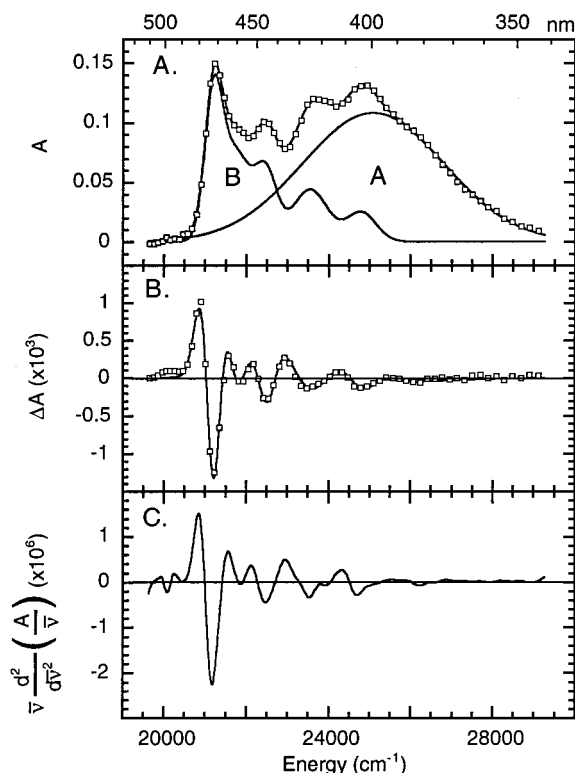


FIG. 2. Absorption Stark spectrum of GFP at 77 K. (*A*) The absorption spectrum. (*B*) The Stark spectrum (change in absorption upon application of an 0.6 MV/cm electric field). (*C*) The analytical second derivative of the absorption spectrum. The close similarity between the Stark and second derivative lineshapes for the lower energy transition indicates that its Stark effect is dominated by a change in dipole moment. The simultaneous best fits of the absorption spectrum and Stark spectrum using this second derivative are shown in *A* and *B*. This permits deconvolution of the broad, higher energy absorption, as shown in *A*. This band does not contribute to the Stark spectrum because it is so broad.

sion anisotropy over the 500–600 nm region is 0.25 and 0.27 for excitation at 398 nm and 478 nm, respectively. Excitation at 398 nm produces higher anisotropy in the wavelength region between 420 and 470 nm and a dip in the anisotropy centered at 485 nm. The room temperature fluorescence spectra of GFP-D excited at either peak are indistinguishable from those of GFP (data not shown) indicating that exchanging protons with deuterium has no effect on the protein or chromophore structure.

In contrast to room temperature, the steady-state fluorescence profile at 77 K depends strongly on the excitation energy as shown in Fig. 3. Excitation of the low energy feature at 471 nm generates emission peaked at 482 nm (Fig. 3C). As the excitation energy increases, the emission spectrum changes: a prominent band around 504 nm emerges, and the peak at 482 nm becomes relatively less intense. Steady-state fluorescence spectra taken at 25° intervals show that, following A and B state excitation, the peak of the emission shifts to higher energy by 250 and 1000 cm^{-1} , respectively, as the temperature is lowered from room temperature to 77 K (data not shown). The emission anisotropy spectra for excitation at the same wavelengths are shown in the subpanels in Fig. 3. Excitation at 471 nm produces a constant anisotropy value of 0.28 across the emission spectrum. As the excitation energy increases, the anisotropy of the 482 nm band decreases significantly. The dashed traces in Fig. 3 show the dramatic effect of deuterating exchangeable protons on the steady-state fluorescence spectrum at 77 K. Excitation of GFP-D at high energy (404 nm, Fig.

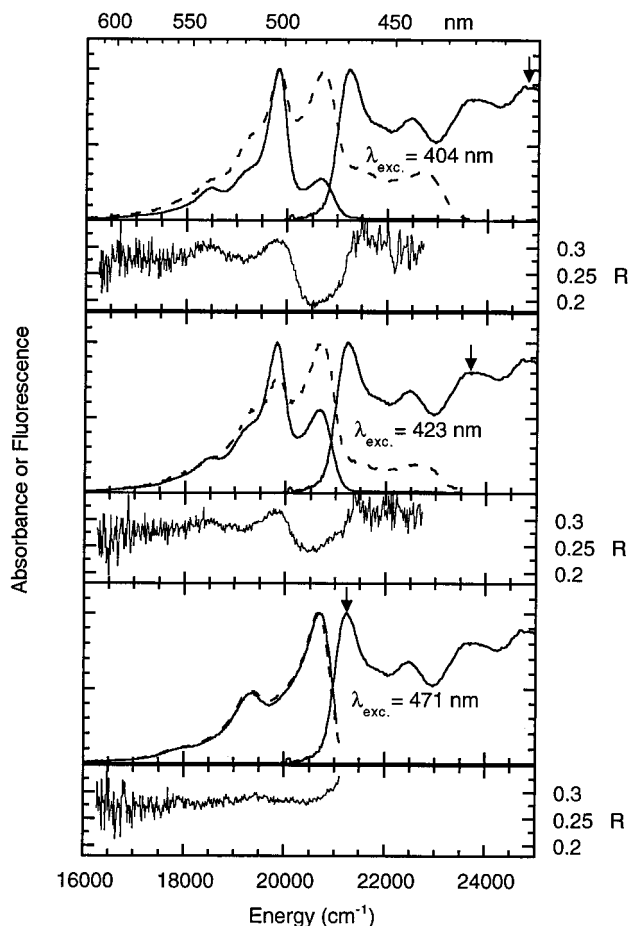


Fig. 3. Steady state fluorescence emission of GFP (—) and GFP-D (---) at 77 K excited at 404 nm, 423 nm, and 471 nm. The absorption spectrum is shown for comparison in each panel (the absorption spectra of GFP and GFP-D are identical). The subpanels show the corresponding steady-state fluorescence anisotropy, $R = (I_{\parallel} - I_{\perp}) / (I_{\parallel} + 2I_{\perp})$, for GFP excited at the same wavelengths.

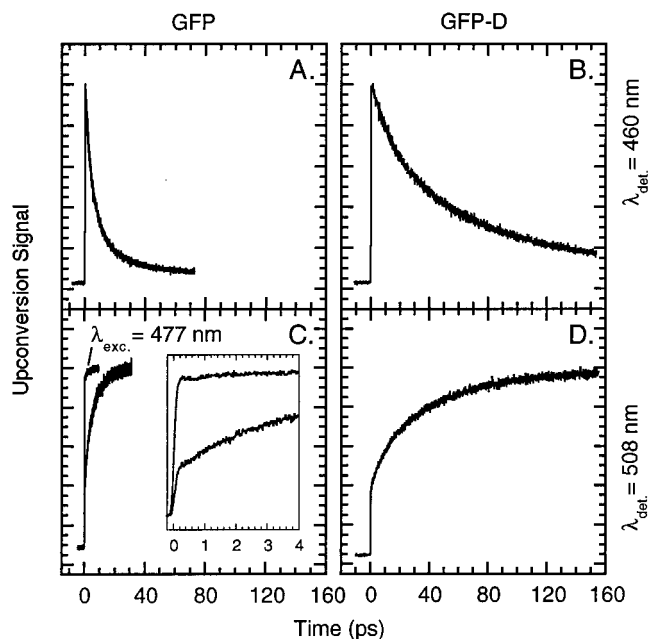


Fig. 4. Room temperature time-resolved fluorescence of GFP (A and C) and GFP-D (B and D) excited into the higher energy absorption band at 398 nm and detected at either 460 nm (emission from A^* , panels A and B) or 508 nm (panels C and D). The effect of direct excitation of the lower energy band at 477 nm detected at 508 nm is also shown in C. The inset to C shows the first few ps of the kinetics on an expanded time base. The total counts actually detected at the maximum of the upconversion signal were: (A) 2,648 counts, (B) 2,891 counts, (C) 5,099 counts (398 nm excitation) and 21,529 counts (477 nm excitation), (D) 9,031 counts.

3A) produces emission at 504 nm, also the dominant emission for protonated GFP, as well as relatively more emission at 482 nm than in the protonated sample. In addition, emission features that are barely detectable in the protonated sample between 420 and 470 nm are observed. By contrast, selective excitation of the lower energy band at 471 nm yields fluorescence spectra that are independent of isotopic composition (Fig. 3C).

Excited State Kinetics. To untangle the excited state dynamics suggested by the steady-state fluorescence data at low temperature and upon deuteration of exchangeable protons, we measured the early time emission at room temperature following excitation of the high and low energy bands as shown in Fig. 4. Direct excitation of the lowest energy band at 478 nm at room temperature leads to an instantaneous (within the instrument response) appearance of emission at 508 nm (Fig. 4C).[‡] This emission persists out to 150 ps (the longest time observed), with only a small decay over this timescale [the fluorescence lifetime of GFP is 3.3 ns at room temperature (3)]. By contrast, as shown in Fig. 4A, when GFP is excited into the higher energy absorption at 398 nm and the emission from this state is monitored at 460 nm, there is a rapid decay of the excited state population. The kinetics of this decay match the rise in the amplitude of the emission from the lower energy state at 508 nm (Fig. 4C). As seen in the inset to Fig. 4C, a fraction of the emission at 508 nm following 398 nm excitation is instantaneous and is due to direct excitation of the underlying absorption from the lower energy state (c.f., Figs. 1 and 2A).

[‡]Close inspection of the first ps of this emission (Fig. 4C inset) reveals a small-amplitude oscillation. Such oscillations are often observed in the spontaneous emission from systems that are excited impulsively with very short pulses and are due to vibrational coherence (15).

Table 1. Lifetimes τ and amplitudes for the decay components of the excited state of GFP and GFP-D at room temperature

	Excitation	Emission	Amplitude	τ , ps
CFP	398 nm (25,125 cm ⁻¹)	460 nm (21,740 cm ⁻¹)	0.50 ± 0.03 0.40 ± 0.05 0.10 ± 0.01	3.6 ± 0.3 12.0 ± 1.0 120.0 ± 15.0
	398 nm (25,125 cm ⁻¹)	508 nm (19,685 cm ⁻¹)	-0.24 ± 0.02 -0.43 ± 0.03	2.2 ± 0.2 8.1 ± 0.5
	478 nm (20,920 cm ⁻¹)	508 nm (19,685 cm ⁻¹)	-0.06 ± 0.01	1.9 ± 0.2
	398 nm (25,125 cm ⁻¹)	460 nm (21,745 cm ⁻¹)	0.46 ± 0.02 0.54 ± 0.02	22.0 ± 0.4 116.0 ± 2.0
GFP-D	398 nm (25,125 cm ⁻¹)	508 nm (19,685 cm ⁻¹)	-0.16 ± 0.01 -0.49 ± 0.02	8.2 ± 0.5 46.0 ± 3.0
	478 nm (20,920 cm ⁻¹)	508 nm (19,685 cm ⁻¹)	-0.07 ± 0.005	1.9 ± 0.2

A negative amplitude implies an initial rise in emission intensity prior to the decay.

Deuteration has a dramatic effect on the excited state dynamics at room temperature as shown in Fig. 4 *B* and *D*. The excited state decay following excitation of the higher energy transition monitored at 460 nm slows substantially. This is matched by a comparable slowing in the rise in fluorescence detected at 508 nm, which builds on an instantaneous component due to direct excitation of the overlapping lower energy band (see Fig. 2*A*). To evaluate possible mechanisms for the large isotope effect, we need a quantitative model for the data. In most cases the decay or rise could be well fit by a sum of exponentials, although in no case were the kinetics well described by a single exponential process. The results of such an analysis are summarized in Table 1. Alternatively, we can compare the decay of the higher excited state for GFP and GFP-D from the relative area under the curves in Fig. 4 *A* and *B*; this gives a value of about five for the kinetic isotope effect. The 460-nm decay for both GFP and GFP-D also exhibits a second, longer time constant that is not manifest in the rise of the 508 nm emission.

It is difficult to obtain upconversion data at low temperature, so only limited information is available. Fig. 5 shows the temperature dependence of the fluorescence decay at 460 nm following excitation at 398 nm. The decay slows as the temperature is lowered, until at 85 K, following an instantaneous component, the fluorescence *rises* on the tens of ps timescale.

Photoconversion. It has been known for some time that the absorption spectrum of GFP in the visible region changes upon exposure to light with wavelengths 400 nm or shorter.⁸ This photoconversion process complicates applications of GFP in fluorescence imaging. On exposure of dark-adapted GFP to 398-nm laser light, the absorbance of the high energy band slowly diminishes, and there is a concomitant increase in the absorbance of the lower energy band, shown in Fig. 6. After resting for 24 hr in the dark, a substantial fraction of the photoconverted GFP relaxes back toward equilibrium. Both the forward photoconversion and dark relaxation exhibit an isobestic point at 425 nm. The ratio of the change in absorbance of band B (centered at 478 nm) to the change of band A (centered at 398 nm) is a factor of two. Excitation at 478 nm also results in an increase in the absorbance of band B and a decrease in the absorbance of band A. Note that even at this low energy there is some overlap of the absorption of A and B (Fig. 1), which leads to the rise in absorbance at 478 nm upon prolonged excitation with light of this wavelength, i.e., population A is being converted to population B.

⁸Tsien, R. Y., *Fluorescent Proteins and Applications Conference*, March 6, 1995, Palo Alto, CA.

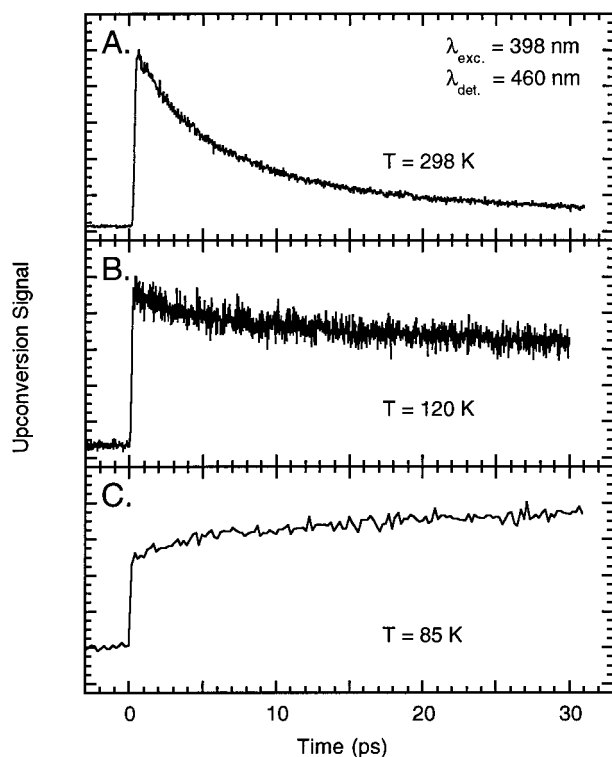


Fig. 5. Temperature dependence of the time-resolved emission of GFP excited into the higher energy band at 398 nm and detected at 460 nm (emission from A^{*}). (A) Room temperature, (B) 120 K, (C) 85 K. The total counts actually detected at the maximum of the upconversion signal were: (A) 2648 counts, (B) 714 counts, (C) 1943 counts.

DISCUSSION

Two limiting models can be used to explain the data presented here and by previous workers. The two electronic transitions corresponding to excitation at 478 and 398 nm at room temperature could arise from transitions between a common ground state and the first and second electronic excited states of a single chromophore, or they could correspond to the excitation of separate species that are capable of interconverting, both in the ground and excited states. We will argue that all of the data fit well with the second model with the further suggestion, based on the effects of deuteration, that the excited state conversion process involves proton transfer.

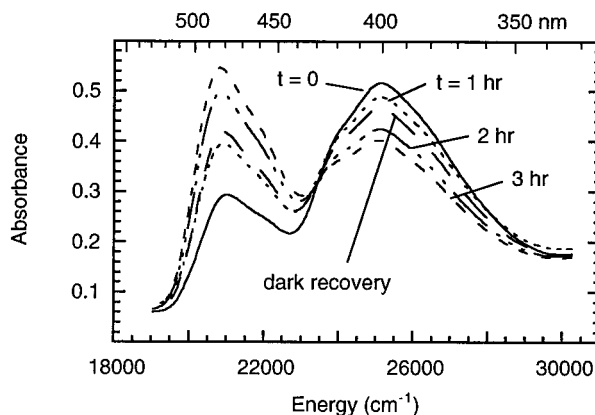


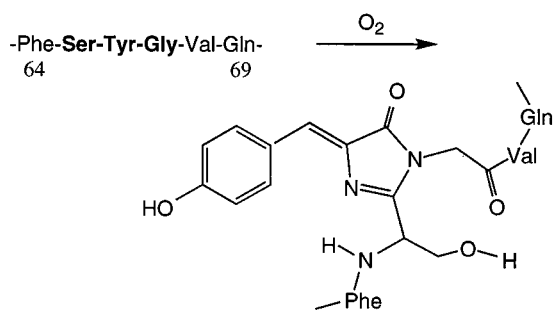
Fig. 6. The effect of irradiation with laser light at 398 nm on the absorption spectrum of GFP at room temperature showing the loss of absorbance of the 398-nm species A band and increase of the 478-nm species B band over several hours. This photoconversion process reverses slowly in the dark, e.g., the spectrum taken 24 hr after cessation of irradiation has recovered about 60%.

We consider the ground state first. The relative intensity of the two peaks in the visible absorption spectrum of GFP is sensitive to pH, temperature, ionic strength, protein concentration (4), and exposure to light, all involving continuous and reversible changes with well-defined isobestic points indicative of two interconvertible populations in equilibrium (see e.g., Fig. 6). This suggests that GFP exists in two ground-state forms, called A and B, whose relative populations are sensitive to the environment. The photoconversion data show that the extinction coefficient of band B is about two times that of band A. Before excitation, the absorbance of band B is about one-third that of band A. Therefore, the ground-state population of state B is approximately one-sixth that of state A, suggesting that the ground state of A is lower in energy. Since relaxation after excited state photoconversion takes hours at room temperature (Fig. 6), the barrier to the $B \rightarrow A$ ground-state conversion is large.

When B is excited directly at room temperature (e.g., at 477 nm), the fluorescence from B^* at 508 nm rises immediately and does not decay appreciably during the time window sampled by the fluorescence upconversion experiment (Fig. 4C). At low temperature, direct excitation of B gives structured steady-state fluorescence, which roughly mirrors the absorption and is independent of the protonation state of the GFP (Fig. 3C). Upon excitation into higher vibrational states of B^* , the anisotropy of the associated emission drops considerably (Fig. 3A and B). Up to this point, the photophysics of state B is unexceptional.

As the excitation energy is increased and state A absorption begins to dominate, the time evolution of the excited state becomes more complicated, and it depends on temperature and isotopic composition. When excited at 398 nm at room temperature A^* decays rapidly to form another excited species, as seen by the rapid decay of emission characteristic of A^* at 460 nm and the corresponding rise of the emission at 508 nm (Fig. 4A and C). Although it is tempting to associate this emission with B^* , that is, to consider it to be from the same species created by direct excitation of B, the situation is somewhat more complex. Specifically, the photoconversion of A into B via A^* is not an efficient process, whereas the excited state decay of A^* into another excited species seen in Fig. 4A and C is a very rapid and efficient process. Therefore, there must be an intermediate state, which we designate I. As described below, I is likely a form of B with corresponding excited state I^* . As the temperature is lowered, the decay of A^* slows, and at 85 K the emission does not decay at all during the 30 ps window shown in Fig. 5C, suggesting that a barrier exists to the $A^* \rightarrow I^*$ process. The steady-state fluorescence data demonstrate that this process also depends on isotopic composition at low temperature as there is substantially more emission in the 460 nm region for GFP-D than GFP at 77 K (Fig. 3A).

It is appropriate at this point to speculate on the characteristics that differentiate species A, I, and B, the nature of the A^* decay process, and how this relates to the photoconversion process. We stress that time-resolved emission data cannot uniquely resolve these questions, although it can exclude some possibilities. The chromophore responsible for the green fluorescence has been characterized by Cody *et al.* (2) and is believed to be:



The observation that the visible absorption spectrum of GFP is strongly and reversibly influenced by pH (4) gives credence to the view that species A and B differ in protonation state. There are several sites within the chromophore that could accept or donate a proton, and the transfer could occur within the chromophore or between the chromophore and a nearby residue of the protein. The data clearly show that the electronic state accessed by excitation of GFP at 398 nm undergoes a nonradiative decay to another electronic state whose emission maximum is 5500 cm^{-1} lower in energy, and that this decay exhibits a strong isotope effect involving exchangeable protons. Thus, the A^* decay process is strongly coupled to proton motion. Since the seminal work on excited state proton transfer by Kasha and coworkers (17), many examples have been reported. Because A^* decay is very fast, but leads only rarely to ground state species B (the forward photoconversion process illustrated in Fig. 6), there must be a process that rapidly regenerates the ground state of species A. If the primary decay of A^* were $A^* \rightarrow B^* \rightarrow B$, then the sample would rapidly be converted to species B, because species B relaxes back to species A very slowly (the reverse process illustrated in Fig. 6). Thus, we propose an intermediate B-like species denoted I and suggest that A^* decays rapidly to I^* , which can either emit a photon returning to I or undergo (rarely) the further evolution to B^* . As the emission from I^* is very similar to that from B^* when B is directly excited at room temperature, we propose that I^* and I are unrelaxed forms of B^* and B, respectively. Once I^* has returned to its ground state, it rapidly converts back to species A or (rarely) evolves further to species B. This phenomenology is illustrated schematically in Fig. 7. A possible model to explain this is that the solvent (protein) around I^* and I relaxes in stages and relatively slowly to form B^* and B, respectively. Thus, I is electronically like species B, but environmentally like species A. Then, just as the excited state conversion of A^* to I^* is very rapid and involves proton transfer, the reverse ground-state conversion of I to A can be very rapid (we have no information on how rapid, but we observe that the absorption of species A is not bleached during its high repetition rate excitation at 398 nm). The molecular nature of the relaxation process that converts I^* or I to B^* or B, respectively, is not known, but it may be similar to solvation dynamics following charge displacement (in this case proton transfer), which have been extensively studied in simple solvents (18) and proteins (19). If the solvation of I is slower than back proton transfer to A, then fully solvated I, which we call B, is only rarely formed, but once formed can only relax slowly to species A. In contrast to simple solvents where solvation is very fast, solvation in a protein occurs much more slowly and over many time scales (19). In light of this

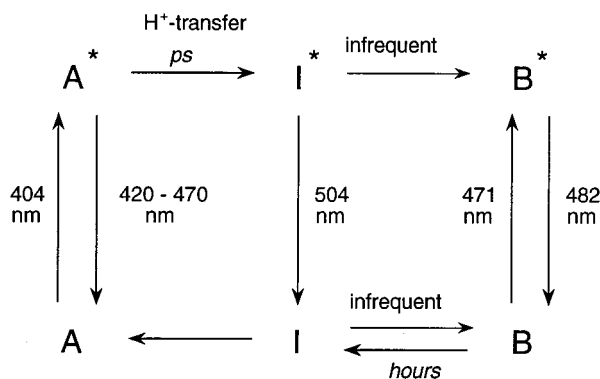


FIG. 7. Reaction scheme that is consistent with the absorption and fluorescence spectra, observed excited dynamics, effect of deuterating exchangeable protons, and photoconversion process. The indicated wavelengths refer to the spectra at 77 K. As described in the text, the intermediate I is likely an unrelaxed form of species B.

interpretation, it is interesting to note that site directed mutations of Tyr-66 (Y66H, Y66W) produce GFP with only one absorption peak and a blue-shifted room temperature emission spectrum (1), whereas mutations at Ser-65 (e.g., S65T, S65A, S65C) produce GFP with one red-shifted absorption peak and an unchanged room temperature emission spectrum (9, 10). This suggests a link between Tyr-66 and the A state, as well as between Ser-65 and the B state.

High-frequency vibrational modes can act as accepting modes in radiationless transitions between electronic states (20, 21). Deuteration lowers the vibrational frequency, requiring more quanta to be absorbed by this or another mode to take up the excess electronic energy that must be converted to vibrational energy during the transition. This usually leads to weaker coupling between the two electronic states and thus, a lower rate for the transition. Because the decay of A* and rise of I* slows by about a factor of five upon deuteration, it is reasonable to speculate that one or more -OH or -NH stretches constitutes the primary accepting mode(s) and that the A* decay process is an excited state proton transfer reaction. The exact dependence of the rate of this reaction on deuteration is determined by the coupling of the normal mode of the -OH or -NH stretch to the reaction coordinate. As the protein structure is not yet known, there is not any way to further evaluate the molecular origin of the large isotope effect at this time.

The GFP used in this work was prepared with the assistance of Ania Majewska. This work was done at the Stanford Free Electron Laser Center, supported by the Office of Naval Research under Contract N00014-91-C-0170, with additional support from the National Institutes of Health (Grant GM27738). M.C. was a National Institutes of Health Postdoctoral Fellow.

1. Heim, R., Prasher, D. C. & Tsien, R. Y (1994) *Proc. Natl. Acad. Sci. USA* **91**, 12501–12504.

2. Cody, C. W., Prasher, D. C., Westler, W. M., Prendergast, F. G. & Ward, W. W. (1993) *Biochemistry* **32**, 1212–1218.
3. Perozzo, M. A., Ward, K. B., Thompson, R. B. & Ward, W. W. (1988) *J. Biol. Chem.* **263**, 7713–7716.
4. Ward, W. W., Prentice, H. J., Roth, A. F., Cody, C. W. & Reeves, S. C. (1982) *Photochem. Photobiol.* **35**, 803–805.
5. Nageswara Rao, B. D., Kemple, M. D. & Prendergast, F. G. (1980) *Biophys. J.* **32**, 630–632.
6. Bokman, S. H. & Ward, W. W. (1981) *Biochem. Biophys. Res. Commun.* **101**, 1372–1380.
7. Ward, W. W. (1981) in *Bioluminescence and Chemiluminescence: Basic Chemistry and Analytical Applications*, eds. DeLuca, M. A. & McElroy, W. D. (Academic, New York), pp. 235–242.
8. Ward, W. W. & Bokman, S. H. (1982) *Biochemistry* **21**, 4535–4540.
9. Heim, R., Cubitt, A. B. & Tsien, R. Y. (1995) *Nature (London)* **373**, 663–664.
10. Delagrave, S., Hawtin, R. E., Silva, C. M., Yang, M. M. & Youvan, D. C. (1995) *Bio/Technology* **13**, 151–154.
11. Chalfie, M., Tu, Y., Euskirchen, G., Ward, W. W. & Prasher, D. C. (1994) *Science* **263**, 802–805.
12. Grudzinski, H. (1970) *Acta Phys. Pol. A* **37**, 49–66.
13. Boxer, S. G. (1993) in *The Photosynthetic Reaction Center*, eds. Deisenhofer, J. & Norris, J. R. (Academic, New York), Vol. 2, pp. 179–220.
14. Stanley, R. J. & Boxer, S. G. (1995) *J. Phys. Chem.* **99**, 859–863.
15. Mokhtari, A., Chebira, A. & Chesnoy, J. (1990) *J. Opt. Soc. Am. B* **7**, 1551–1557.
16. Ward, W. W., Cody, C. W., Hart, R. C. & Cormier, M. J. (1980) *Photochem. Photobiol.* **31**, 611–615.
17. Taylor, A. T., El-Bayoumi, M. A. & Kasha, M. (1969) *Proc. Natl. Acad. Sci. USA* **63**, 253–260.
18. Maroncelli, M. & Fleming, G. R. (1987) *J. Chem. Phys.* **86**, 6221–6239.
19. Pierce, D. W. & Boxer, S. G. (1992) *J. Phys. Chem.* **96**, 5561–5566.
20. Freed, K. F. (1976) *Top. Appl. Phys.* **15**, 23–168.
21. Lipert, R. J. & Colson, S. D. (1989) *J. Phys. Chem.* **93**, 135–139.